Chemistry–A European Journal
Research Article
doi.org/10.1002/chem.202202408
Chemistry Europe
European Chemical Societies Publishing
www.chemeurj.org

Synthesis of an Antimicrobial Enterobactin-Muraymycin Conjugate for Improved Activity Against Gram-Negative Bacteria

Christian Rohrbacher,[a] Robert Zscherp,[b] Stefanie C. Weck,[a] Philipp Klahn,*[b, c] and Christian Ducho*[a]

Dedicated to Professor Chris Meier on the occasion of his 60th birthday.

Abstract: Overcoming increasing antibiotic resistance requires the development of novel antibacterial agents that address new targets in bacterial cells. Naturally occurring nucleoside antibiotics (such as muraymycins) inhibit the bacterial membrane protein MraY, a clinically unexploited essential enzyme in peptidoglycan (cell wall) biosynthesis. Even though a range of synthetic muraymycin analogues has already been reported, they generally suffer from limited cellular uptake and a lack of activity against Gram-negative bacteria. We herein report an approach to overcome these hurdles: a synthetic muraymycin analogue has been conjugated to a siderophore, i.e. the enterobactin derivative **Ent$_{KL}$**, to increase the cellular uptake into Gram-negative bacteria. The resultant conjugate showed significantly improved antibacterial activity against an efflux-deficient *E. coli* strain, thus providing a proof-of-concept of this novel approach and a starting point for the future optimisation of such conjugates towards potent agents against Gram-negative pathogens.

Introduction

The increasing resistance of bacteria against known antibiotics is an emerging problem. Consequently, the development of new antimicrobial drugs (in particular those addressing novel biological targets) and concepts against bacterial pathogens is of utmost importance.[1] In this context, the development of new antibiotics against Gram-negative pathogens is particularly challenging as the Gram-negative cell envelope comprises an additional outer membrane. This provides a highly effective permeation barrier for many drugs that are otherwise active against Gram-positive bacteria.[2] In addition, enhanced efflux mediated by overexpressed efflux pumps also plays a prominent role in the protection of many Gram-negative microbes against antibacterial action.[3]

An innovative concept to overcome the effective permeation barrier of the Gram-negative cell envelope is to hijack bacterial uptake mechanisms such as their iron uptake machinery. Iron is an essential growth factor for bacteria. In order to ensure their iron supply, they produce and secrete siderophores,[4] i.e. small molecule iron chelators, such as enterobactin (**Ent**, Figure 1) produced by *Escherichia coli*. **Ent** binds iron(III) cations with a remarkably high binding constant. The resultant ferri-**Ent** complex is recognised by specific siderophore receptors in the outer membrane of *E. coli* and then actively transported into the bacterial cytosol. It has been previously demonstrated that appropriate conjugation of antimicrobial drugs to siderophores can enable drug uptake via the

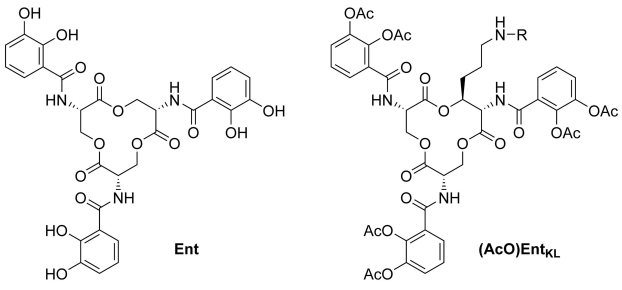

Figure 1. Structures of the siderophore enterobactin (**Ent**) and its novel biomimetic derivative (**AcO**)**Ent$_{KL}$**.

[a] C. Rohrbacher, S. C. Weck, Prof. Dr. C. Ducho
Department of Pharmacy, Pharmaceutical and Medicinal Chemistry
Saarland University
Campus C2 3, 66123 Saarbrücken (Germany)
E-mail: christian.ducho@uni-saarland.de
[b] Dr. des. R. Zscherp, Prof. Dr. P. Klahn
Institute of Organic Chemistry
Technische Universität Braunschweig
Hagenring 30, 38106 Braunschweig (Germany)
[c] Prof. Dr. P. Klahn
Department of Chemistry and Molecular Biology
Division of Organic and Medicinal Chemistry
University of Gothenburg
Kemigården 4, 412 96 Göteborg (Sweden)
E-mail: philipp.klahn@chem.gu.se

Supporting information for this article is available on the WWW under https://doi.org/10.1002/chem.202202408

same pathway in the sense of a 'Trojan Horse' conjugate.[5,6] **Ent** and its glycosylated derivatives are siderophores of *Enterobacteriaceae*[7] and xenosiderophores of the opportunistic human pathogen *Pseudomonas aeruginosa*.[8] They are therefore particularly interesting as carrier units for siderophore-drug conjugates[9] as their high iron-binding constant enables them to dissociate iron from human host proteins, thus providing them with a prominent role during bacterial infection.[10] Recently, we have reported the synthesis and evaluation of the biomimetic enterobactin derivative (**AcO**)**Ent**$_{KL}$ (Figure 1), which has been demonstrated to enable cargo translocation into *E. coli* and *P. aeruginosa*.[11] In order to show that conjugation with (**AcO**)**Ent**$_{KL}$ furnished enhanced antibacterial activity, we aimed to link it to antimicrobial drugs that otherwise lack good activity against Gram-negative bacteria.

In the search for new targets for antibacterial drug discovery, one promising candidate appears to be the enzyme MraY (translocase I). MraY is an integral membrane protein involved in the bacterial peptidoglycan biosynthesis pathway.[12] It catalyses the transfer of UDP-Mur*N*Ac pentapeptide **1** to the lipid carrier undecaprenyl phosphate **2** to furnish peptidoglycan biosynthesis intermediate 'lipid I' **3** (Scheme 1).[13] A class of compounds that inhibit MraY as an antibacterial target are naturally occurring uridine-derived nucleoside antibiotics.[14] One promising sub-class of these natural products are the muraymycins.[15a] In 2002, the isolation of 19 muraymycins from *Streptomyces* sp. was reported.[15b] Since then, several additional muraymycins have been isolated and identified.[15c]

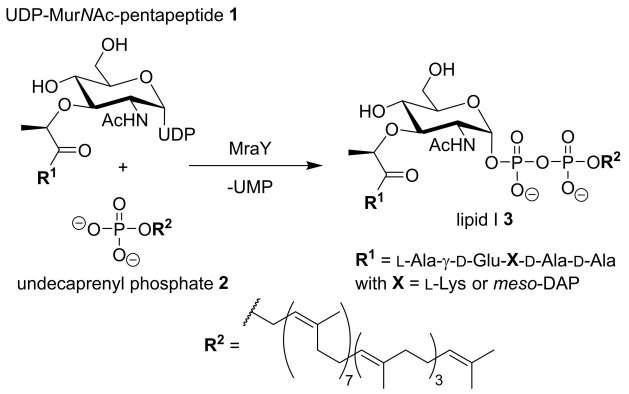

Scheme 1. MraY-catalysed reaction yielding lipid I **3**. UDP = uridine diphosphate, UMP = uridine monophosphate, DAP = 2,6-diaminopimelic acid.

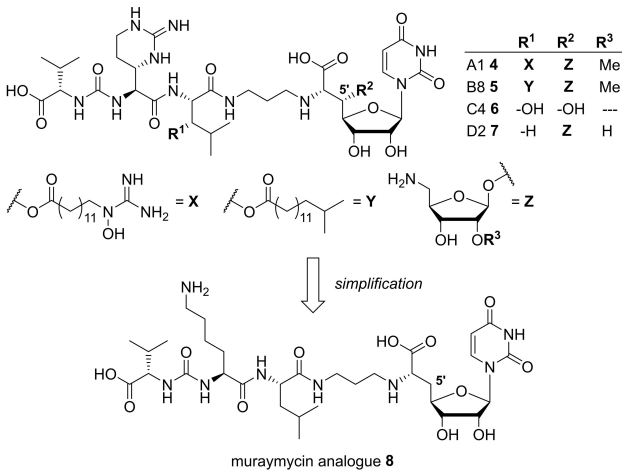

Figure 2. Selected examples **4**–**7** of naturally occurring muraymycins and the structurally simplified synthetic 5′-defunctionalised muraymycin analogue **8**.

Based on the structure of the central L-leucine-derived motif, muraymycins are divided into four subclasses A-D (examples: muraymycins A1 **4**, B8 **5**, C4 **6**, and D2 **7**, Figure 2). All four classes share the 5′-aminoribosylated (5′*S*,6′*S*)-glycyluridine (GlyU) moiety that is connected (via an aminopropyl linker) to a peptide unit containing the L-leucine-derived motif and the arginine-derived amino acid L-epicapreomycidine. Naturally occurring muraymycins, in particular members of the lipophilically acylated A and B series (with structure **R**^{1} being **X** or **Y**, Figure 2), show good activity against Gram-positive bacteria (e.g. *Staphylococci* and *Enterococci*). Representing the current best-in-class natural muraymycin, congener B8 **5** has been reported to be a very potent MraY inhibitor in vitro (IC_{50} = 4.0 ± 0.7 pM) and showed promising antibacterial activity against *S. aureus*.[15c] However, antimicrobial activity of muraymycins against Gram-negative pathogens has only been found for some bacteria, mainly *E. coli* strains with enhanced membrane permeability or deficient efflux, thus hinting at cellular uptake and/or efflux to be delimiters for activity *in bacterio*.[15]]

Muraymycins of the C and D series lacking lipophilic functionalisation generally display much lower antibacterial activities relative to the A and B series derivatives. This beneficial influence of the lipophilic side chain (i.e. structure **R**^{1} being **X** or **Y**, Figure 2) has been studied in more detail using naturally occurring muraymycins as well as artificial model systems.[16] Some naturally occurring muraymycins from the D series have already been obtained by total synthesis,[17] and synthetic methods for individual units of the muraymycin scaffold are available.[18] Numerous synthetic muraymycin analogues have already been reported,[17,19] often based on the rationale to simplify the rather complex structure of the natural products. An X-ray co-crystal structure of MraY (from *Aquifex aeolicus*) in complex with muraymycin D2 **7** was reported in 2016.[20] In combination with a subsequent comprehensive crystallographic study on the interaction of nucleoside antibiotics with MraY,[21] structural insights into the chemical logic of MraY inhibition by muraymycins and related nucleoside antibiotics are now available.

As part of our research on structurally simplified muraymycin analogues, we have established the approach to prepare 5′-defunctionalised ('5′-deoxy') versions of the muraymycin scaffold, i.e. analogues lacking the 5′-aminoribosyl substituent altogether.[22] Though this strategy has led to a loss of inhibitory activity against MraY, resultant analogues were still sufficiently potent as MraY inhibitors and were therefore useful in the context of structure-activity relationship (SAR) studies.[23] One such example of a previously reported '5′-deoxy' muraymycin analogue would be compound **8** (Figure 2) that has the simplified 5′-defunctionalised version of the GlyU core structure

as well as L-lysine as a replacement of the synthetically challenging L-epicapreomycidine unit, thus leading to MraY inhibition in the low μM range ($IC_{50} = 2.5 \pm 0.6$ μM).[23b]

Overall, current knowledge on muraymycin and their analogues strongly suggests that (i) structural variations of the muraymycin scaffold (in the context of simplified analogues) are tolerated; (ii) delimiting factors of their activity *in bacterio* are limited cellular uptake and/or efflux and (iii) the lipophilic fatty acid units in muraymycins of the A and the B series mainly contribute to cellular uptake rather than MraY inhibition, even though a potential lipophilic binding pocket in MraY has been identified.[20,21] Therefore, we aim to identify strategies to further improve bacterial cellular uptake of structurally simplified, chemically tractable muraymycin analogues, also with respect to the long-term goal to improve their activity against Gram-negative pathogens.

One such strategy towards more efficient cellular uptake in Gram-negative bacteria might be the application of the aforementioned 'Trojan Horse' concept, i.e. the conjugation of muraymycin analogues to siderophores. To the best of our knowledge, siderophore conjugates of MraY-inhibiting nucleoside antibiotics are unprecedented. In this work, we report the first proof-of-concept study that this might be a suitable strategy to improve Gram-negative cellular uptake of muraymycin analogues.

Results and Discussion

We first aimed for the synthesis of a novel muraymycin analogue **9** that could be chemically linked to the siderophore unit (**AcO**)**Ent**$_{KL}$. Based on the structure of known analogue **8** (Figure 2), the L-leucine moiety was changed to an L-2,3-diaminopropionic acid (Dap) motif in order to enable the introduction of a thiol-containing side chain. The thiol could then be linked to (**AcO**)**Ent**$_{KL}$ via a disulfide unit. This disulfide motif would be prone to cytosolic cleavage after uptake into bacteria due to the presence of glutathione and oxidoreductases. The design of muraymycin analogue **9** (Scheme 2) was based on the known benefits of a lipophilic side chain in this position of the muraymycin scaffold (see above). It was anticipated that the attached enterobactin structure would function as a transporter system and that intracellular cleavage of the disulfide bond would release **9** as an antibacterially active MraY inhibitor.

For the synthesis of muraymycin analogue **9**, we employed a modified version of our previously reported solid phase-supported approach (Scheme 2).[23c] Linker unit **10** was attached to the 2-chlorotrityl chloride resin under basic conditions to give the functionalised solid phase **11**. After capping of unconverted resin with methanol and DIPEA, the Fmoc-deprotection and peptide coupling sequence started. The first coupling step was carried out with Fmoc-Dap(Cbz)-OH and the

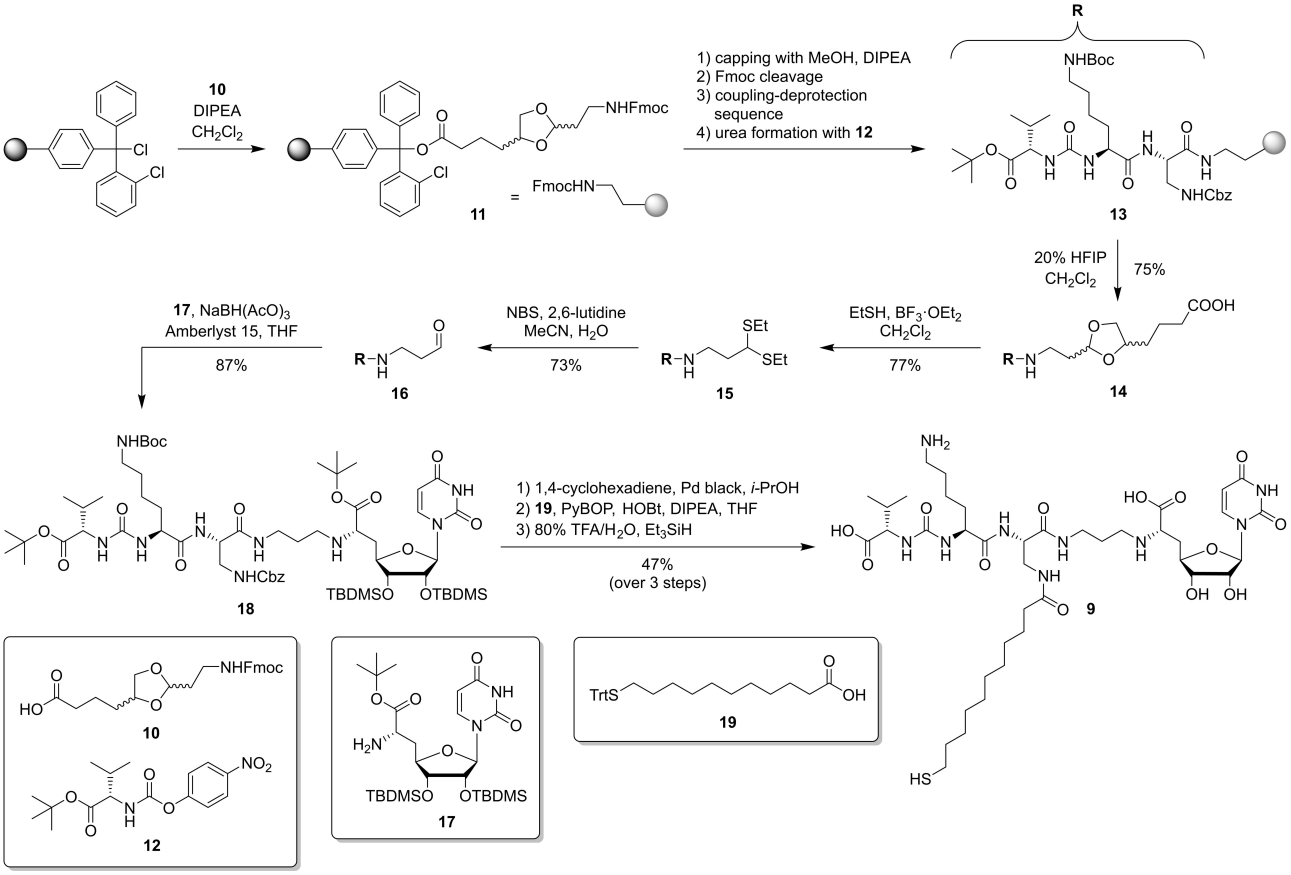

Scheme 2. Solid-phase-supported synthesis of muraymycin analogue **9** for the conjugation reaction. Dap = L-2,3-diaminopropionic acid.

second coupling step with Lys(Boc)-OH. HBTU and DIPEA in DMF were used in each peptide coupling step, and the respective amino acids were used in excess to ensure high conversion. In the final step of the construction of the peptide unit, the urea motif was formed with valine-derived *p*-nitrophenyl carbamate **12** to give **13**. The complete protected peptide unit was cleaved from **13** by mild detritylation with hexafluoroisopropanol, thus affording carboxylic acid **14** in 75% yield over all peptide-forming steps. The 1,3-dioxolane moiety in **14** was transformed into dithioacetal **15** with ethanethiol and boron trifluoride in 77% yield. Subsequently, dithioacetal **15** was converted into aldehyde **16** with NBS and 2,6-lutidine in 73% yield (Scheme 2).

Aldehyde **16** was then used in a reductive amination step with the protected nucleosyl amino acid building block **17**[22b,23c] to afford the protected Dap-containing muraymycin analogue **18** in 87% yield (Scheme 2). After cleavage of the Cbz group in **18** under mild transfer hydrogenation conditions (that helped to avoid unwanted reduction of the uracil C5-C6 double bond[22b]), the resultant partially protected muraymycin analogue could be modified with the side chain unit. Commercially available *S*-trityl-protected 11-mercaptoundecanoic acid **19** was coupled to the Dap-3-amino group under peptide coupling conditions (PyBOP and HOBt in the presence of DIPEA), followed by global acidic deprotection with 80% TFA in water and triethylsilane as scavenger for the trityl group. The deprotection step was carried out under inert gas atmosphere to avoid oxidative disulfide formation. After purification by semi-preparative HPLC, muraymycin analogue **9** was thus obtained in a satisfying yield of 47% over three steps from **18** (Scheme 2). Muraymycin derivative **9** would subsequently serve both as a synthetic building block for conjugate formation and as a reference compound for biological testing.

In order to conjugate antibiotic **9** to the siderophore unit (**AcO**)**Ent$_{KL}$**, the Boc group of its Boc-protected version (**AcO**)**Ent$_{KL}$-Boc**[11] was cleaved in the presence of TFA (Scheme 3). The resultant free amine was coupled with *N*-succinimidyl-3-(2-pyridyldithio)-propionate (SPDP) in a mixture of DMSO and PBS buffer at pH 8.0, thus giving (in 67% yield over two steps) (**AcO**)**Ent$_{KL}$-SSPy** as a synthetic building block with a thiol-reactive 2-pyridinyl disulfide moiety. The final conjugation step of **9** with (**AcO**)**Ent$_{KL}$-SSPy** was achieved in a mixture of DMSO and PBS buffer at pH 7.4, affording the desired target conjugate (**AcO**)**Ent$_{KL}$-SS-9** in 17% yield (Scheme 3).

Both the muraymycin-siderophore conjugate (**AcO**)**Ent$_{KL}$-SS-9** and non-conjugated muraymycin analogue **9** (as a reference compound) were tested for their in vitro inhibitory potency against the bacterial enzyme MraY. For this, an established fluorescence-based activity assay and recombinantly overexpressed MraY (crude membranes of overexpressing *E. coli* cells) were used.[16a,24] This assay gave similar IC_{50} values of 123 ± 7 nM for the conjugate (**AcO**)**Ent$_{KL}$-SS-9** and 68 ± 4 nM for non-conjugated muraymycin analogue **9**, respectively (Table 1), thus suggesting that they both were strong, equally potent MraY inhibitors. As crude bacterial membranes were employed in the assay, one should take into account that reducing agents (mainly other thiols) probably were present in the assay mixtures. Hence, the conjugate (**AcO**)**Ent$_{KL}$-SS-9** might have been cleaved to the muraymycin analogue **9** and the enterobactin-derived thiol (**AcO**)**Ent$_{KL}$-SH** under these conditions. The inhibitory activity of the rather bulky compound (**AcO**)**Ent$_{KL}$-SS-9** would then be owed to the partially released muraymycin analogue **9**.

In order to further study this aspect, we have repeated the MraY assay with conjugate (**AcO**)**Ent$_{KL}$-SS-9**, but including

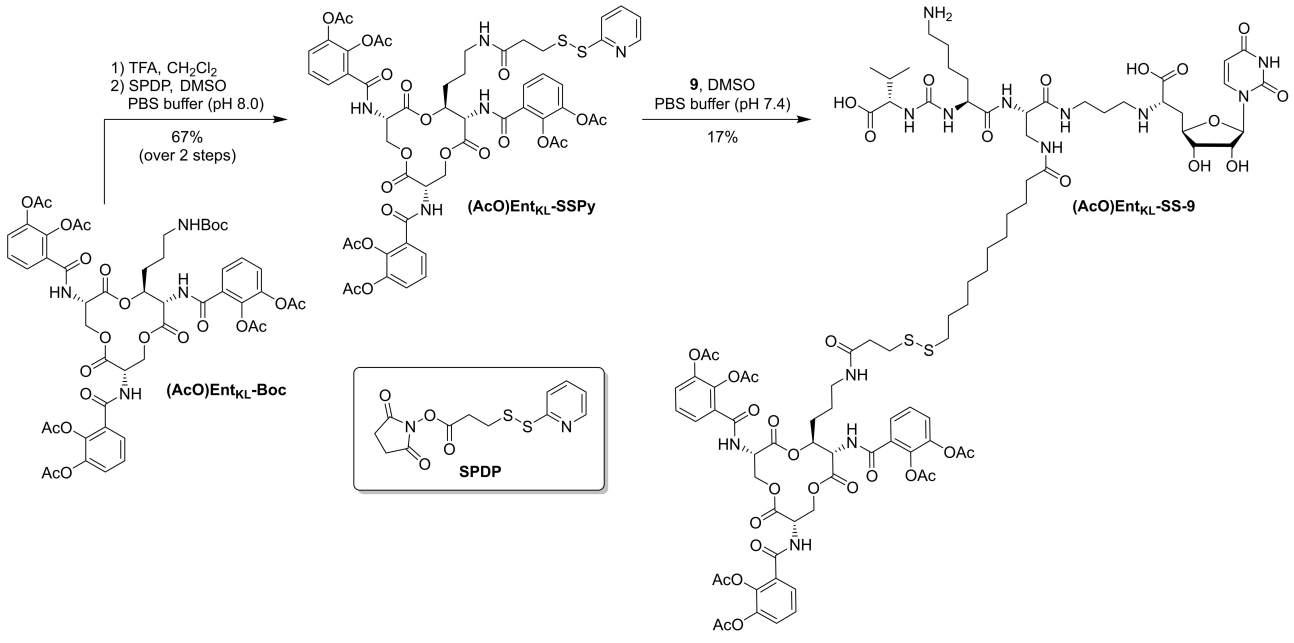

Scheme 3. Synthesis of the muraymycin-siderophore conjugate (**AcO**)**Ent$_{KL}$-SS-9**. SPDP = *N*-succinimidyl-3-(2-pyridyldithio)-propionate.

Table 1. Biological activities of the muraymycin-enterobactin conjugate (**AcO**)**Ent$_{KL}$-SS-9** and non-conjugated muraymycin analogue **9**.

Compound	MraY inhibition in vitro[a] IC_{50} [nM]	Antibacterial activities[b] IC_{50} (*E. coli* Δ*tolC*) [μM]	IC_{50} (*E. coli* DH5α) [μg/mL]	IC_{50} (*P. aeruginosa* PAO1) [μg/mL]
9	68 ± 4	23 ± 6	> 100	> 100
(AcO)Ent$_{KL}$-SS-9	123 ± 7 (89 ± 11)[c]	2.0 ± 1.7	> 100	> 100

[a] Fluorescence-based in vitro MraY inhibition assay with crude membranes of overexpressing cells, IC_{50} ± SD. [b] Growth inhibition of the respective bacterial strain (measured by optical density at 600 nm), IC_{50} ± SD. [c] MraY inhibition assay with crude membranes after treatment of the membrane preparation with 1 mM diamide.

treatment of the membrane preparation with 1 mM diamide. Diamide can be used to efficiently oxidise thiols to disulfides.[25] Hence, a diamide-treated membrane preparation should be free of reducing thiols and therefore leave the disulfide linkage in conjugate (**AcO**)**Ent$_{KL}$-SS-9** intact. The MraY activity of diamide-preincubated membranes in the absence of inhibitors was not significantly different from regular MraY preparations (data not shown), which validated this approach. Remarkably, the MraY assay including diamide treatment gave a nearly identical result for MraY inhibition by (**AcO**)**Ent$_{KL}$-SS-9** (IC_{50} = 89 ± 11 nM, Table 1). This suggested that MraY was indeed potently inhibited in vitro by the intact full-length conjugate (**AcO**)**Ent$_{KL}$-SS-9** rather than by muraymycin analogue **9** as its cleavage product. It cannot be excluded though that **9** contributes to MraY inhibition *in bacterio*.

The strong (nM) inhibitory activity of 5′-defunctionalised muraymycin analogue **9** was remarkable as previously reported analogue **8** had been a ca. 37-fold weaker MraY inhibitor (IC_{50} = 2.5 ± 0.6 μM, see above). This boost in inhibitory in vitro activity against MraY can probably be attributed to hydrophobic interactions of the undecanoyl side chain with the lipophilic pocket in MraY (see above), thus challenging the previous hypothesis that such fatty acid motifs mainly contribute to cellular uptake of muraymycins rather than their target interaction.

It cannot be fully excluded that the fatty acid unit mediates membrane localisation rather than displaying an additional interaction with MraY, as accumulation at the membrane interface should also lead to increased in vitro activity against MraY. However, the proven hydrophobic interactions of other types of lipophilically functionalised nucleoside antibiotics with MraY[21] strongly suggest that a similar effect should also be responsible for the improved inhibitory activity of muraymycin analogue **9**.

Both the muraymycin-enterobactin conjugate (**AcO**)**Ent$_{KL}$-SS-9** and muraymycin analogue **9** (as reference) were also evaluated for their antibacterial activities, i.e. their potential to inhibit bacterial growth. These activities *in bacterio* were measured as IC_{50} values (i.e. concentrations leading to 50% growth inhibition) rather than MIC values (i.e. minimal inhibitory concentrations) as we anticipated that this would enable a more precise quantitative comparison of activities of different compounds (MIC values are commonly determined using two-fold dilution steps). Against the efflux-competent *E. coli* DH5α strain, there was no significant activity observed for both compounds (IC_{50} > 100 μg/mL, Table 1). This was not surprising as naturally occurring muraymycins had previously been found to be inactive against this *E. coli* strain.[16a] Both substances were also tested against an efflux-deficient *E. coli* strain without a functional gene encoding the TolC efflux pump (*E. coli* Δ*tolC*). Against this strain, the reference muraymycin **9** already showed moderate growth inhibition (IC_{50} = 23 ± 6 μM, Table 1). With the attachment of the enterobactin unit (**AcO**)**Ent$_{KL}$** in conjugate (**AcO**)**Ent$_{KL}$-SS-9**, a ca. 11-fold increase of antibacterial activity was observed (IC_{50} = 2.0 ± 1.7 μM, Table 1).

In our previous work, the enterobactin derivative (**AcO**)**Ent$_{KL}$** had already been tested for its biological properties and had shown no signs of antibacterial activity.[11] Hence, the observed activity of the muraymycin conjugate (**AcO**)**Ent$_{KL}$-SS-9** is an unambiguous indication of an improved cellular uptake of the muraymycin analogue **9**. It can be assumed that a similar initial enhancement of cellular uptake might also occur in the *E. coli* DH5α strain, but the efficient efflux mechanisms in this strain probably prevent an intracellular accumulation of **9** that would be sufficient for growth inhibition. Again, these data are fully consistent with previous findings as naturally occurring muraymycins had been found to display strong growth inhibition against *E. coli* Δ*tolC*, with the differences to the DH5α strain indicating that efflux from *E. coli* might be a delimiter of antibacterial activity for this class of antibiotics. The remarkable antibacterial activity of (**AcO**)**Ent$_{KL}$-SS-9** against *E. coli* Δ*tolC* (in contrast to *E. coli* DH5α) shows that improved cellular uptake is not sufficient to compensate for competing efflux mechanisms in *E. coli*, but it still demonstrates a successful intracellular delivery of **9**. The ca. 11-fold improvement in antibacterial activity (against *E. coli* Δ*tolC*) resulting from the attachment of the enterobactin unit is unprecedented for conjugates with (**AcO**)**Ent$_{KL}$**[11] and suggests that MraY-inhibiting nucleoside antibiotics might be a suitable class of compounds for the design of such conjugates. The detected moderate activity of **9** against *E. coli* Δ*tolC* is also noteworthy as previously reported muraymycin analogue **8** had shown no significant growth inhibition against this strain.[23b] This improved antibacterial activity of **9** (relative to **8**) might be owed to enhanced cellular uptake of **9** (as a result of its lipophilic functionalisation) or to its more potent inhibition of MraY (see above).

Naturally occurring muraymycins are generally not active against the Gram-negative pathogen *P. aeruginosa*.[15] Hence, it was anticipated that both conjugate (**AcO**)**Ent$_{KL}$-SS-9** and muraymycin analogue **9** might lack activity against the growth of the *P. aeruginosa* PAO1 strain, and this was indeed observed (IC_{50} > 100 μg/mL for both compounds, Table 1). A recent study

demonstrates that the activity of some subclasses of nucleoside antibiotics (i.e. mureidomycins and related structures) against *P. aeruginosa* is strongly related to protein-mediated active transport specific for these subclasses and some of their analogues.[26] Siderophore conjugation might not be sufficient to mediate a similarly efficient effect on uptake into *P. aeruginosa*. In addition, efflux-related phenomena in *P. aeruginosa* PAO1 are also very likely to play a role.

The lack of antibacterial activity of (**AcO**)**Ent$_{KL}$**-**SS**-**9** against *E. coli* DH5α and *P. aeruginosa* showed that such conjugates will require further optimisation in order to display a broader spectrum of activity against Gram-negative bacteria. One approach for future optimisation might be the conjugation of enterobactin units to inherently more potent MraY inhibitors. Many naturally occurring muraymycins inhibit MraY in the pM range,[16a] and therefore, lower intracellular concentrations (relative to **9**) should furnish antibacterial activity. Improved cellular uptake of such extremely potent MraY inhibitors due to siderophore conjugation might therefore be sufficient to outcompete efflux and achieve antibacterial activity. The synthesis of muraymycin analogues that are structurally very closely related to the parent natural products and that are also functionalised for conjugation reactions will be chemically more challenging though. In principle, the muraymycin unit in (**AcO**)**Ent$_{KL}$**-**SS**-**9** could also be replaced with other nucleoside antibiotics, for instance, representatives of subclasses with inherent activity against *P. aeruginosa* (see above).[14,15a,26] An alternative approach to overcome efflux as a delimiter of antibacterial activity might be the exchange of the bioreversible disulfide linker with intracellularly stable structures (e.g. a triazole unit). Thus, the parent nucleoside antibiotic would not be released inside the bacterial cell, and as a result, efflux might be significantly slower or even fully prevented. However, the intact conjugate would then need to inhibit the target enzyme MraY. Our results reported herein (see above) indicate that this might be potentially feasible.

Conclusion

In summary, we herein report the synthesis and biological evaluation of an unprecedented muraymycin-enterobactin conjugate (**AcO**)**Ent$_{KL}$**-**SS**-**9**. In order to obtain this conjugate, we have employed a solid-phase-supported synthesis of the muraymycin peptide unit for an efficient preparation of novel muraymycin analogue **9**. This natural product analogue was then connected to the siderophore moiety (**AcO**)**Ent$_{KL}$** by formation of a bioreversible disulfide linker.

Both muraymycin analogue **9** and its enterobactin conjugate (**AcO**)**Ent$_{KL}$**-**SS**-**9** displayed remarkably strong inhibitory potencies against the bacterial target protein MraY in vitro. Conjugate (**AcO**)**Ent$_{KL}$**-**SS**-**9** showed a pronounced improvement (ca. 11-fold) of antibacterial activity against the efflux-deficient *E. coli* Δ*tolC* strain relative to **9**. This provided a proof-of-concept that siderophore conjugation might become a valuable approach to enhance the antibacterial activities of MraY-inhibiting nucleoside antibiotics such as **9** against Gram-negative pathogens.

However, the lack of antibacterial activity of (**AcO**)**Ent$_{KL}$**-**SS**-**9** against an efflux-competent *E. coli* strain and *P. aeruginosa* (with efflux likely playing an important role in both cases) also demonstrated that such conjugates will require further optimisation to achieve a broader spectrum of activity against Gram-negative bacteria. The proof-of-concept reported herein suggests approaches for this optimisation effort, mainly to exchange the muraymycin and linker units to alternative structures. Work along this line is on the way in our laboratories.

Experimental Section

General methods: All chemicals were purchased from standard suppliers and used without further purification. Linker unit **10**,[23c] *p*-nitrophenyl carbamate **12**,[23c] nucleoside building block **17**,[22b] and enterobactin derivative (**AcO**)**Ent$_{KL}$**-**Boc**[11] were synthesised as previously reported. All air- and/or water-sensitive reactions were performed under inert gas atmosphere (nitrogen or argon, dried over orange gel and phosphorus pentoxide) with anhydrous solvents. All glassware used for these reactions was dried by heating under vacuum. THF, DMF and CH_2Cl_2 were purchased in HPLC quality and dried with a solvent purification system (MBRAUN MB SPS 800). Anhydrous DMSO and *i*-PrOH were purchased and additionally dried over activated molecular sieve (4 Å). All other solvents were of technical quality and freshly distilled before use, and deionised water was used throughout. Reaction monitoring was carried out by TLC, LC-MS or NMR spectroscopy. Aluminium plates precoated with silica gel 60 F_{254} (VWR) or glass plates precoated with silica gel 60 F_{254} (Merck) were used for TLC. Spots were detected by UV light (254 or 366 nm) and/or staining under heating with VSS TLC stain (4.0 g vanillin, 25 mL H_2SO_4 (conc.), 80 mL AcOH, all dissolved in MeOH (680 mL)), CAM TLC stain (1.0 g Ce(IV)$(SO_4)_2$, 2.5 g $(NH_4)_6Mo_4O_7$ in 100 mL 10% H_2SO_4) or ninhydrin solution (0.3 g ninhydrin, 3 mL AcOH, all dissolved in 100 mL 1-butanol). For column chromatography, silica gel 60 (40–63 μm, 230–400 mesh ASTM, VWR) was used. Semipreparative HPLC was performed on two different systems: i) an Agilent Technologies 1200 Series system equipped with an MWD detector and a LiChroCART® 250–10 Purospher® STAR RP-18 endcapped (5 μm) column or a Macherey-Nagel VP 250/10 NUCLEODUR phenyl-hexyl (5 μm) column; method 1: eluent A water (+0.1% TFA), eluent B MeCN (+0.1% TFA); 0–3 min 0% B, 3–25 min gradient of B (0–80%), 25–32 min gradient of B (80–100%), 32–40 min 100% B, 40–41 min gradient of B (100–40%), 41–45 min gradient of B (40–0%), flow 2.0 mL/min, UV/vis detector (254 nm, 260 nm); ii) a Thermo Fisher Scientific Dionex Ultimate 3000 HPLC system with a UV/vis detector and Hypersil GOLD C18 RP-column (Part No. 25005–259070 A, 5 μm, 250 mm×10 mm) equipped with a guard column of the same material; method 2: eluent A 10 mM NH_4OAc in water, eluent B MeCN; 0–30 min gradient of B (20–95%), 30–35 min 95% B, 35–40 min gradient of B (95–20%), 40–45 min 20% B, flow 5 mL/min, UV/vis detector (220 nm). NMR spectra were recorded on different NMR spectrometers from Bruker. For ^{1}H NMR spectra at 500 MHz and ^{13}C NMR spectra at 126 MHz, a Bruker Avance I 500 or a Bruker AVIIIHD500 with cryoprobe system were used. The ^{1}H NMR spectra at 300 MHz and ^{13}C NMR spectra at 75 MHz were recorded on a Bruker Fourier 300 or a Bruker AV-300. For ^{1}H NMR spectra recorded at 400 MHz as well as ^{19}F NMR spectra at 376 MHz, a Bruker Avance II 400 was used. Chemical shifts (δ) are quoted in ppm. Coupling constants (*J*) are reported in Hz. The signals were

assigned using ^{1}H,^{1}H-COSY, ^{1}H,^{13}C-HSQC and ^{1}H,^{13}C-HMBC spectra. All ^{13}C NMR spectra are ^{1}H-decoupled. All spectra were recorded at room temperature and referenced internally to solvent reference frequencies. Low-resolution mass spectra were measured on an LC-MS system consisting of an Accela HPLC (Thermo Scientific) equipped with an Accela photodiode array (PDA) detector, Accela autosampler, and Accela 1250 pump that was coupled to an LTQ XL mass spectrometer (Thermo Scientific) for HPLC/HESI-MS analyses. Heated electrospray ionisation was used with an enhanced scan range of 120 to 2000 amu. Gradient HPLC solvent programs consisted of LC-MS-grade water, MeCN, and 2% HCOOH in water. An Agilent Zorbax Eclipse Plus C18 (3.5 μm, 2.1×150 mm) column was used at 30 °C. The PDA detector was set to a scanning range from 190 to 600 nm with 1 nm wavelength steps. High-resolution mass spectra were measured on three different systems: i) a Thermo Scientific Q Exactive Orbitrap mass spectrometer with ESI ionisation mode and a Thermo Scientific Ultimate 3000 HPLC system (Thermo Accucore™ phenyl-X column (2.1 μm, 3×100 mm)); ii) a Finnigan MAT 95 (EI, 70 eV) mass spectrometer; iii) a Finnigan MAT 95 XL (ESI) mass spectrometer. UV/vis spectra were recorded on an Agilent Cary 100 or on a Cary 100 Bio (Varian) spectrophotometer. For HPLC-purified substances, the absorption maxima from DAD data were used. The wavelengths of the absorption maxima are given in nm. For infrared spectroscopy, a Bruker Fourier-transform infrared (FTIR) spectrometer ALPHA with an integrated PlatinumATR™ unit or Bruker Tensor 27 IR spectrometer with ATR technology were used, and wavenumbers are quoted in cm^{-1}. A Krüss P3000 polarimeter ($\lambda = 589$ nm) was used at rt to record specific optical rotations.

Thiol-functionalised muraymycin analogue (**9**): For Cbz deprotection, muraymycin analogue **18** (52 mg, 40 μmol), Pd black (10 mg, 94 μmol) and 1,4-cyclohexadiene (0.10 mL, 86 mg, 1.1 μmol) were dissolved in *i*-PrOH (8 mL) and stirred at rt for 4 h. After filtration, the solvent was evaporated under reduced pressured. The resultant product was obtained as a colourless solid (47 mg) and was used in the next step without further purification. *S*-trityl-11-mercaptoundecanoic acid **19** (34 mg, 74 μmol), PyBOP (39 mg, 74 μmol), HOBt (10 mg, 74 μmol) and DIPEA (26 μL, 0.14 mmol) were dissolved in THF (10 mL) and the mixture was stirred at rt for 15 min. After addition of a solution of the Cbz-deprotected muraymycin analogue (85 mg, 74 μmol) in THF (5 mL), the reaction mixture was stirred at rt for 17 h. The solvent was evaporated under reduced pressure and the resultant crude product was purified by column chromatography (CH_2Cl_2-MeOH, 98:2→95:5). The thus obtained protected muraymycin analogue (15 mg, 9.4 μmol) and triethylsilane (2.3 mg, 3.0 μL, 19 μmol) were dissolved in degassed TFA and water (4:1, 8 mL) and stirred at rt for 20 h. The reaction mixture was then diluted with water (15 mL, degassed) and lyophilized. The resultant crude product was purified by semipreparative HPLC (method 1) to give **9** (bis-TFA salt) as a colourless foam (5.7 mg, 47% over 3 steps from **18**). ^{1}H NMR (500 MHz, D_2O): $\delta = 0.91$ (d, J = 6.8 Hz, 3H, Val-4-H), 0.93 (d, $J = 6.8$ Hz, 3H, Val-4-H), 1.13–1.26 (m, 10H, alkyl-4-H, alkyl-5-H, alkyl-6-H, alkyl-7-H, alkyl-8-H), 1.26–1.34 (m, 2H, alkyl-9-H), 1.34–1.45 (m, 2H, Lys-4-H), 1.45–1.58 (m, 4H, alkyl-3-H, alkyl-10-H), 1.58–1.71 (m, 3H, Lys-3-H_a, Lys-5-H), 1.72–1.81 (m, 1H, Lys-3-H_b), 1.82–1.93 (m, 2H, 2''-H), 2.06–2.14 (m, 1H, Val-3-H), 2.14–2.20 (m, 2H, alkyl-2-H), 2.20–2.28 (m, 1H, 5'-H_a), 2.34–2.43 (m, 1H, 5'-H_b), 2.48 (t, $J = 6.6$ Hz, 2H, alkyl-11-H), 2.95 (t, $J = 7.3$ Hz, 2H, Lys-6-H), 3.04 (t, $J = 6.9$ Hz, 2H, 1''-H), 3.12–3.21 (m, 1H, 3''-H_a), 3.24–3.34 (m, 1H, 3''-H_b), 3.39–3.49 (m, 1H, Dap-3-H_a), 3.53–3.62 (m, 1H, Dap-3-H_b), 3.81–3.90 (m, 1H, 6'-H), 3.96–4.07 (m, 3H, 3'–H, Val-2-H, Lys-2-H), 4.08–4.16 (m, 1H, 4'-H), 4.30–4.36 (m, 1H, Dap-2-H), 4.36–4.41 (m, 1H, 2'-H), 5.71 (d, $J = 3.2$ Hz, 1H, 1'-H), 5.83 (d, $J = 8.2$ Hz, 1H, 5-H), 7.61 (d, $J = 8.2$ Hz, 1H, 6-H) ppm. ^{13}C NMR (126 MHz, D_2O): δ = 17.27 (Val-C-4), 18.68 (Val-C-4), 21.97 (Lys-C-4), 23.92 (alkyl-C-11), 25.45 (C-2''), 26.17 (alkyl-C-3), 27.76, 28.47, 28.51, 28.55, 28.88, 29.15, 29.56 (alkyl-C-4, alkyl-C-5, alkyl-C-6, alkyl-C-7, alkyl-C-8, alkyl-C-9, Lys-C-5), 30.00 (Val-C-3), 30.63 (Lys-C-3), 32.80 (C-5'), 33.34 (alkyl-C-10), 35.64 (C-3''), 36.07 (alkyl-C-2), 39.10 (Lys-C-6), 40.17 (Dap-C-3), 44.10 (C-1''), 54.52 (Lys-C-2), 54.70 (Dap-C-2), 58.80 (Val-C-2), 59.62 (C-6'), 72.63 (C-2'), 72.84 (C-3'), 79.85 (C-4'), 91.51 (C-1'), 102.10 (C-5), 116.28 (q, $^{1}J_{CF} = 292.5$ Hz, $F_3\underline{C}COO$), 142.60 (C-6), 151.25 (C-2), 159.61 (N(C=O)N), 162.84 (q, $^{2}J_{CF} = 35.4$ Hz, $F_3C\underline{C}OO$), 165.97 (C-4), 171.40 (C-7'), 171.96 (alkyl-C-1), 175.60 (Dap-C-1), 176.38 (Lys-C-1), 177.79 (Val-C-1) ppm. ^{19}F NMR (376 MHz, D_2O): $\delta = -75.56$ (TFA-CF_3) ppm. HRMS (ESI): calcd. for $C_{40}H_{69}N_9O_{13}S$ $[M+2H]^{2+}$ 458.7441, found 458.7418. IR (ATR): $\nu = 3287$, 3078, 2927, 2855, 1643, 1555, 1199, 1131, 720, 549 cm^{-1}. UV (HPLC): $\lambda_{max} = 202$, 261 nm. HPLC (method 1): $t_R = 22.9$ min.

SPPS of Val-Lys-Dap peptide unit (**14**): Solid phase-supported synthesis of the peptide unit was in principle performed as reported before.[23c] 2-Chlorotrityl chloride resin (130 mg, 0.141 mmol) was loaded into a syringe equipped with a filter frit and swollen with CH_2Cl_2 for 1–2 h. Linker unit **10**[23c] (70.0 mg, 0.165 mmol) and DIPEA (75.0 μL, 54.5 mg, 0.422 mmol) in CH_2Cl_2 (3 mL) were loaded into the syringe and shaken for 21.5 h at rt. Fmoc deprotection was carried out with 20% piperidine in DMF (4 mL) at rt for 20 min. The solution was then filtered and the resin washed with CH_2Cl_2 and DMF (5×4 mL each two times). Fmoc-DAP(Z)-OH (195 mg, 0.423 mmol) was coupled using HBTU (160 mg, 0.422 mmol) and DIPEA (150 μL, 109 mg, 0.846 mmol) in CH_2Cl_2 (4 mL) at rt for 22 h. After Fmoc deprotection, coupling with Fmoc-Lys(Boc)-OH (198 mg, 0.423 mmol) was carried out with HBTU (160 mg, 0.422 mmol) and DIPEA (150 μL, 109 mg, 0.846 mmol) in CH_2Cl_2 (4 mL) at rt for 23 h. *Tert*-butyl ((4-nitrophenoxy)carbonyl)-L-valinate **12**[23c] (120 mg, 0.355 mmol) and DIPEA (150 μL, 109 mg, 0.846 mmol) in CH_2Cl_2 (4 mL) were loaded and shaken at rt for 21 h. The fully assembled peptide unit was then cleaved from the solid phase with a solution of 20% HFIP in CH_2Cl_2 (4 mL) and shaking at rt for 15 min. The resin was washed with CH_2Cl_2 (15–20 x, 4 mL each) and the solvent was evaporated under reduced pressure. The resultant crude product was purified by column chromatography (CH_2Cl_2-MeOH, 95:5) to give **14** (mixture of 1,3-dioxolane diastereomers) as a colourless solid (89.9 mg, 75% over all peptide-forming steps). ^{1}H NMR (500 MHz, CD_3OD): $\delta = 0.91$ (d, $J = 6.9$ Hz, 3H, Val-4-H), 0.94 (d, $J = 6.9$ Hz, 3H, Val-4-H), 1.28–1.53 (m, 4H, Lys-4-H, 3'-H), 1.43 (s, 9H, Boc-OC(CH_3)$_3$), 1.47 (s, 9H, C(CH_3)$_3$), 1.54–1.68 (m, 4H, Lys-5-H, 4'-H), 1.69–1.79 (m, 2H, Lys-3-H), 1.79–1.90 (m, 2H, 2-H), 2.03–2.13 (m, 1H, Val-3-H), 2.28–2.33 (m, 2H, 5'-H), 3.03 (t, J = 6.8 Hz, 2H, Lys-6-H), 3.22–3.34 (m, 2H, 3-H), 3.38–3.59 (m, 3H, Dap-3-H, 1'-H_a), 3.90 (dd, $J = 7.3$ Hz, 1H, 2'-H), 3.98–4.13 (m, 3H, Val-2-H, Lys-2-H, 1'-H_b), 4.37–4.42 (m, 1H, Dap-2-H), 4.91–5.02 (m, 1H, 1-H), 5.04–5.14 (m, 2H, Cbz-CH_2), 7.27–7.40 (m, 5H, Cbz-aryl-H) ppm. MS (ESI): $m/z = 851.61$ $[M+H]^+$. HRMS (ESI): calcd. for $C_{41}H_{66}N_6O_{13}$ $[M-H]^-$ 849.4615, found 849.4598. IR (ATR): $\nu = 3297$, 2933, 2873, 1692, 1631, 1541, 1366, 1252, 1141, 696 cm^{-1}. UV (*i*-PrOH): $\lambda_{max} = 217$ nm. TLC (CH_2Cl_2-MeOH, 9:1): $R_f = 0.27$.

Val-Lys-Dap peptide dithioacetal (**15**): Val-Lys-Dap peptide 1,3-dioxolane **14** (200 mg, 0.236 mmol) and ethanethiol (0.26 mL, 0.22 g, 3.5 mmol) were dissolved in CH_2Cl_2 (40 mL). After addition of boron trifluoride diethyl etherate (2.0 μL, 16 μmol, dissolved in 2 mL CH_2Cl_2), the solution was stirred at rt for 6 d. DIPEA (0.14 mL, 0.11 mg, 0.82 mmol) was added and the reaction mixture was stirred for 5 min. The solvents were evaporated under reduced pressure and the resultant crude product was purified by flash column chromatography (CH_2Cl_2-MeOH, 98:2) to give **15** as a colourless solid (151 mg, 77%). ^{1}H NMR (500 MHz, $CDCl_3$): $\delta = 0.85$ (d, $J = 6.6$ Hz, 3H, Val-4-H), 0.91 (d, $J = 6.9$ Hz, 3H, Val-4-H), 1.24 (t, $J = 7.4$ Hz, 6H, H-2'), 1.31–1.41 (m, 2H, Lys-4-H), 1.40–1.49 (m, 2H, Lys-5-H), 1.46 (s, 18H, Boc-OC(CH_3)$_3$, OC(CH_3)$_3$), 1.64–1.74 (m, 1H, Lys-3-H_a), 1.74–1.83 (m, 1H, Lys-3-H_b), 1.95–2.05 (m, 2H, H-2), 2.10

(dd, $J=11.8$, 6.5 Hz, 1H, Val-3-H), 2.53–2.73 (m, 4H, 1′-H), 2.99–3.18 (m, 2H, Lys-6-H), 3.25–3.33 (m, 1H, 3-H_a), 3.50–3.61 (m, 3H, 3-H_b, Dap-3-H), 3.85 (t, $J=7.1$ Hz, 1H, 1-H), 4.00–4.08 (m, 1H, Lys-2-H), 4.34 (dd, $J=8.7$, 4.6 Hz, 1H, Val-2-H), 4.46–4.53 (m, 1H, Dap-2-H), 4.88–4.96 (m, 1H, Boc-NH), 4.99–5.16 (m, 2H, Cbz-CH_2), 5.64–5.73 (m, 2H, Val-NH, Dap-3-NH), 5.95–6.03 (m, 1H, Lys-NH), 7.28–7.38 (m, 5H, Cbz-aryl-H), 7.50–7.56 (m, 1H, 3-NH), 7.61 (d, $J=7.6$ Hz, 1H, Dap-2-NH) ppm. ^{13}C NMR (126 MHz, $CDCl_3$): $\delta=14.45$ (C-2′), 17.39 (Val-C-4), 19.04 (Val-C-4), 21.95 (Lys-C-4), 24.14 (C-1′), 24.26 (C-1′), 28.04 (OC($\underline{C}H_3)_3$), 28.51 (Boc-OC($\underline{C}H_3)_3$), 29.74 (Lys-C-5), 30.59 (Val-C-3), 31.54 (Lys-C-3), 35.35 (C-2), 37.75 (C-3), 39.29 (Lys-C-6), 42.45 (Dap-C-3), 48.73 (C-1), 54.93 (Dap-C-2), 55.47 (Lys-C-2), 58.09 (Val-C-2), 66.89 (Cbz-CH_2), 79.34 (Boc-O$\underline{C}(CH_3)_3$), 81.84 (O$\underline{C}(CH_3)_3$), 127.75 (Cbz-C-2), 128.14 (Cbz-C-4), 128.51 (Cbz-C-3), 136.17 (Cbz-C-1), 156.67 (Cbz-C=O), 157.94 (Boc-C=O), 158.46 (N(C=O)N), 169.74 (Lys-C-1), 172.10 (Dap-C-1), 173.47 (Val-C-1) ppm. HRMS (ESI): calcd. for $C_{39}H_{66}N_6O_9S_2$ $[M+H]^+$ 827.4406, found 827.4398. IR (ATR): $\nu=3289$, 2931, 1694, 1629, 1539, 1366, 1267, 1158, 695, 641 cm^{-1}. UV (MeOH): $\lambda_{max}=206$ nm. TLC (CH_2Cl_2-MeOH, 9:1) $R_f=0.57$.

Val-Lys-Dap peptide aldehyde (**16**): Val-Lys-Dap peptide dithioacetal **15** (205 mg, 0.248 mmol) was dissolved in a mixture of MeCN, water and acetone (8:2:1, 40 mL) and cooled to 0 °C. 2,6-Lutidine (425 mg, 460 μL, 3.97 mmol) and NBS (352 mg, 1.98 mmol) were added at this temperature and the reaction mixture was stirred at 0 °C for 7 min. Subsequently, sat. $Na_2S_2O_3$ solution (60 mL) was added and the mixture was stirred at rt for 4 min. The aqueous layer was extracted with CH_2Cl_2 (3×120 mL). The combined organics were dried over Na_2SO_4 and the solvent was evaporated under reduced pressure. The resultant crude product was purified by flash column chromatography (CH_2Cl_2-MeOH, 95:5) to give **16** as a colourless solid (131 mg, 73%). ^{1}H NMR (500 MHz, $CDCl_3$): $\delta=0.85$ (d, $J=6.9$ Hz, 3H, Val-4-H), 0.91 (d, $J=6.9$ Hz, 3H, Val-4-H), 1.18–1.48 (m, 4H, Lys-4-H, Lys-5-H), 1.45 (s, 9H, Boc-OC($CH_3)_3$), 1.46 (s, 9H, OC($CH_3)_3$), 1.62–1.85 (m, 2H, Lys-3-H), 1.98–2.15 (m, 1H, Val-3-H), 2.66 (t, $J=6.1$ Hz, 2H, 2-H), 2.98–3.19 (m, 2H, Lys-6-H), 3.27–3.39 (m, 1H, Dap-3-H_a), 3.42–3.50 (m, 1H, 3-H_a), 3.50–3.62 (m, 2H, 3-H_b, Dap-3-H_b), 4.04–4.14 (m, 1H, Lys-2-H), 4.29 (dd, $J=8.2$, 4.1 Hz, 1H, Val-2-H), 4.47–4.55 (m, 1H, Dap-2-H), 4.99 (bs, 1H, Boc-NH), 5.00–5.14 (m, 2H, Cbz-CH_2), 5.72–5.85 (m, 2H, Val-NH, Dap-3-NH), 6.05–6.13 (m, 1H, Lys-NH), 7.28–7.40 (m, 5H, Cbz-aryl-H), 7.62–7.69 (m, 1H, 3-NH), 7.70 (d, $J=7.6$ Hz, 1H, Dap-2-NH), 9.73 (s, 1H, 1-H) ppm. ^{13}C NMR (126 MHz, $CDCl_3$): $\delta=17.49$ (Val-C-4), 18.99 (Val-C-4), 22.02 (Lys-C-4), 28.04 (OC($\underline{C}H_3)_3$), 28.50 (Boc-OC($\underline{C}H_3)_3$), 29.67 (Lys-C-5), 30.89 (Val-C-3), 31.47 (Lys-C-3), 33.31 (C-3), 39.38 (Lys-C-6), 42.36 (Dap-C-3), 43.31 (C-2), 54.82 (Dap-C-2), 55.35 (Lys-C-2), 58.22 (Val-C-2), 66.85 (Cbz-CH_2), 79.27 (Boc-O$\underline{C}(CH_3)_3$), 81.84 (O$\underline{C}(CH_3)_3$), 127.77 (Cbz-C-2), 128.11 (Cbz-C-4), 128.50 (Cbz-C-3), 136.26 (Cbz-C-1), 156.64 (Cbz-C=O), 157.85 (Boc-C=O), 158.54 (N(C=O)N), 170.06 (Lys-C-1), 172.10 (Dap-C-1), 173.57 (Val-C-1), 201.01 (C-1) ppm. HRMS (ESI): calcd. for $C_{35}H_{56}N_6O_{10}$ $[M+H]^+$ 721.4131, found 721.4110. IR (ATR): $\nu=3295$, 2972, 2932, 1693, 1679, 1630, 1540, 1257, 1158, 753 cm^{-1}. UV (MeOH): $\lambda_{max}=209$ nm. TLC (CH_2Cl_2-MeOH, 9:1): $R_f=0.35$.

Cbz-protected muraymycin analogue (**18**): Val-Lys-Dap peptide aldehyde **16** (130 mg, 0.180 mmol) and nucleosyl amino acid building block **17**[22b] (106 mg, 0.180 mmol) were dissolved in dry THF (22 mL) over molecular sieve (4 Å) and stirred at rt for 25 h. Amberlyst™ 15 (8.4 mg, 39 μmol) and sodium triacetoxyborohydride (80 mg, 0.38 mmol) were added and the reaction mixture was stirred at rt for 24 h. It was then filtered and the residue was washed with EtOAc. The solvent of the filtrate was evaporated under reduced pressure and the resultant crude product was purified by flash column chromatography (CH_2Cl_2-MeOH, 98:2→95:5) to give **18** as a colourless solid (204 mg, 87%). ^{1}H NMR (500 MHz, CD_3OD): $\delta=0.08$ (s, 3H, $SiCH_3$), 0.10 (s, 3H, $SiCH_3$), 0.12 (s, 3H, $SiCH_3$), 0.13 (s, 3H, $SiCH_3$), 0.91 (s, 9H SiC($CH_3)_3$), 0.93 (s, 9H, SiC($CH_3)_3$), 0.84–0.97 (m, 6H, Val-4-H), 1.25–1.52 (m, 4H, Lys-4-H, Lys-5-H), 1.43 (s, 9H, Boc-OC($CH_3)_3$), 1.48 (s, 9H, OC($CH_3)_3$), 1.49 (s, 9H, OC($CH_3)_3$), 1.53–1.80 (m, 4H, Lys-3-H, 2″-H), 1.89–2.14 (m, 3H, 5′-H, Val-3-H), 2.55–2.72 (m, 2H, 1″-H), 3.03 (t, $J=6.8$ Hz, 2H, Lys-6-H), 3.12–3.19 (m, 1H, 3″-H_a), 3.32–3.38 (m, 1H, 3″-H_b), 3.39–3.53 (m, 3H, Dap-3-H, 6′-H), 3.92 (dd, $J=4.4$, 4.4 Hz, 1H, 3′-H), 4.01 (dd, $J=8.2$, 5.0 Hz, 1H, Lys-2-H), 4.05–4.12 (m, 2H, Val-2-H, 4′-H), 4.33–4.42 (m, 2H, 2′-H, Dap-2-H), 5.04–5.15 (m, 2H, Cbz-CH_2), 5.73–5.75 (m, 1H, 1′-H), 5.75 (d, $J=7.9$ Hz, 1H, 5-H), 7.26–7.39 (m, 5H, Cbz-aryl-H), 7.65 (d, $J=7.9$ Hz, 1H, 6-H) ppm. ^{13}C NMR (126 MHz, CD_3OD): $\delta=-4.29$ ($SiCH_3$), −4.24 ($SiCH_3$), −4.24 ($SiCH_3$), −3.85 ($SiCH_3$), 18.19 (Val-C-4), 19.03 (Si$\underline{C}(CH_3)_3$), 19.10 (Si$\underline{C}(CH_3)_3$), 19.83 (Val-C-4), 24.23 (Lys-C-4), 26.55 (SiC($\underline{C}H_3)_3$), 26.61 (SiC($\underline{C}H_3)_3$), 28.52 (Boc-OC($\underline{C}H_3)_3$), 28.60 (OC($\underline{C}H_3)_3$), 28.98 (OC($\underline{C}H_3)_3$), 30.00 (Lys-C-5), 30.76 (C-2″), 32.45 (Val-C-3), 32.98 (Lys-C-3), 37.72 (C-5′), 38.27 (C-3″), 41.27 (Lys-C-6), 43.40 (Dap-C-3), 45.91 (C-1″), 56.32 (Lys-C-2), 56.44 (Dap-C-2), 60.14 (Val-C-2), 60.57 (C-6′), 67.85 (Cbz-CH_2), 75.79 (C-2′), 76.73 (C-3′), 80.00 (C-4′), 82.68 (O$\underline{C}(CH_3)_3$), 82.79 (O$\underline{C}(CH_3)_3$), 83.40 (Boc-O$\underline{C}(CH_3)_3$), 92.49 (C-1′), 103.19 (C-5), 128.88 (Cbz-C-2), 129.21 (Cbz-C-4), 129.67 (Cbz-C-3), 138.28 (Cbz-C-1), 143.23 (C-6), 152.27 (C-2), 158.66 (Boc-C=O), 159.81 (Cbz-C=O), 160.81 (N(C=O)N), 166.22 (C-4), 172.10 (C-7′), 173.35 (Lys-C-1, Dap-C-1), 176.05 (Val-C-1) ppm. MS (ESI): *m/z*= 1290.56 $[M+H]^+$. HRMS (ESI): calcd. for $C_{62}H_{107}N_9O_{16}Si_2$ $[M+H]^+$ 1290.7447, found 1290.7431. IR (ATR): $\nu=3304$, 2930, 2857, 1691, 1536, 1366, 1250, 1152, 837, 776 cm^{-1}. UV (MeOH): $\lambda_{max}=260$ nm. TLC (CH_2Cl_2-MeOH, 9:1): $R_f=0.39$.

(**AcO**)**Ent$_{KL}$-SSPy**: TFA (100 μL, 1.31 mmol) was added to a solution of (**AcO**)**Ent$_{KL}$-Boc**[11] (6.2 mg, 5.7 μmol) in CH_2Cl_2 (500 μL) at 0 °C and the resultant mixture was stirred at 23 °C for 35 min. The mixture was then co-evaporated with toluene (3×3 mL) and concentrated under reduced pressure. The resultant residue was dissolved in DMSO (80 μL) and PBS buffer (pH 8.0, 20 μL), and *N*-succinimidyl-3-(2-pyridyldithio)-propionate (SPDP, 2.7 mg, 8.6 μmol) was added at 23 °C. The reaction mixture was stirred at 23 °C for 90 min. It was then evaporated under reduced pressure and the resultant residue was purified by flash column chromatography (CH_2Cl_2-MeOH, 92.5:7.5) to give (**AcO**)**Ent$_{KL}$-SSPy** as a colourless amorphous solid (4.9 mg, 67% over 2 steps from (**AcO**)**Ent$_{KL}$-Boc**). ^{1}H NMR (300 MHz, $CDCl_3$): $\delta=8.43$ (ddd, $J=4.8$, 1.7, 1.0 Hz, 1H), 7.85–7.47 (m, 8H), 7.31–7.25 (m, 4H), 7.15–7.05 (m, 2H), 6.68 (t, $J=6.1$ Hz, 1H), 5.45–5.27 (m, 1H), 5.16–5.07 (m, 1H), 4.95 (dt, $J=7.6$, 3.9 Hz, 1H), 4.86 (dd, $J=7.7$, 5.2 Hz, 1H), 4.74 (ddd, $J=36.6$, 11.5, 4.0 Hz, 1H), 4.38 (dd, $J=11.6$, 3.8 Hz, 1H), 4.22 (dd, $J=11.4$, 4.7 Hz, 1H), 3.53–3.46 (m, 1H), 3.20–3.16 (m, 1H), 2.95–2.84 (m, 2H), 2.56–2.39 (m, 2H), 2.36–2.08 (m, 18H), 1.93 (q, $J=7.2$ Hz, 2H), 1.36–1.29 (m, 4H) ppm. ^{13}C NMR (126 MHz, $CDCl_3$): $\delta=171.29$, 170.21, 169.40, 169.07, 169.01, 168.94, 168.77, 168.39, 168.33, 168.31, 168.25, 168.21, 165.48, 165.31, 165.20, 143.15, 143.03, 140.95, 140.71, 128.93, 128.89, 128.73, 127.68, 127.58, 127.19, 126.85, 126.79, 126.63, 126.59, 126.49, 126.47, 126.39, 126.25, 124.83, 118.43, 115.52, 115.33, 115.20, 65.29, 56.57, 38.66, 37.25, 34.89, 34.58, 32.09, 29.86, 29.82, 29.52, 22.85, 20.93, 20.83, 20.76, 20.74, 20.66, 14.27 ppm. MS (ESI): *m/z*=1176.24 $[M+H]^+$. HRMS (ESI): calcd. for $C_{53}H_{53}N_5NaO_{22}S_2$ $[M+Na]^+$ 1198.2516, found 1198.2524. IR (ATR): $\nu=3345$, 2926, 2858, 1752, 1693, 1531, 1693, 1531, 1456, 1386, 1254, 1203, 1169, 1109, 1017, 881, 797, 655, 588 cm^{-1}. TLC (CH_2Cl_2-MeOH, 92.5:7.5): $R_f=0.32$.

Conjugate (**AcO**)**Ent$_{KL}$-SS-9**: Thiol-functionalised muraymycin analogue **9** (bis-TFA salt, 1.8 mg, 2.0 μmol) was added to a solution of (**AcO**)**Ent$_{KL}$-SSPy** (1.8 mg, 1.5 μmol) in DMSO (150 μL) and PBS buffer (pH 7.4, 30 μL) and the reaction mixture was stirred at 23 °C for 2 h. It was then diluted with MeCN and water (1:1, 500 μL), filtered through a CHROMAFIL® 45 μm filter and directly purified by semipreparative HPLC (method 2). Product-containing fractions were diluted with water and lyophilised to give (**AcO**)**Ent$_{KL}$-SS-9** as

a colourless amorphous solid (0.5 mg, 17%). ^{1}H NMR (500 MHz, $CDCl_3$): δ = 7.95–7.24 (m, 10H), 7.15–7.03 (m, 4H), 5.52–5.26 (m, 4H), 5.13–4.10 (m, 12H), 4.02–3.07 (m, 5H), 2.56 (s, 2H), 2.35–2.13 (m, 20H), 2.09–2.00 (m, 10H), 1.92–1.30 (m, 40H), 1.07–0.86 (m, 10H). MS (ESI): *m/z* = 1980.48 $[M+H]^+$, 991.28 $[M+2H]^{2+}$. HRMS (ESI): calcd. for $C_{88}H_{117}N_{13}Na_2O_{35}S_2$ $[M+2Na]^{2+}$ 1013.3517, found 1013.3520. IR (ATR): ν = 3367, 3297, 2924, 2854, 2338, 1771, 1662, 1533, 1460, 1372, 1258, 1204, 1167, 1077, 1018, 970, 908, 802, 729, 597, 586, 574 cm^{-1}. TLC (CH_2Cl_2-MeOH, 9:1): R_f = 0.00. HPLC (method 2): t_R = 18.0 min.

MraY assay: The overexpression of MraY and the fluorescence-based assay for MraY activity (in the absence of diamide) were performed as described before.[16a,24d] In brief, a crude membrane preparation of MraY from *S. aureus* (1 μL, final overall protein concentration ~1 mg/mL)[16a,24d] was added to a mixture of undecaprenyl phosphate (50 μM), dansylated Park's nucleotide (7.5 μM)[24d] and the tested compound in buffer (100 mM Tris-HCl buffer pH 7.5, 200 mM KCl, 10 mM $MgCl_2$, 0.1% Triton X-100, 20 μL overall). For assays with diamide-treated MraY-containing crude membranes, this protocol was modified as follows. A concentrated stock solution of MraY-containing crude membranes (overall protein concentration ~40 mg/mL) was diluted with an equal volume of a stock solution of diamide in water (2 mM). The resultant mixture (overall protein concentration ~20 mg/mL, 1 mM diamide) was incubated at 0 °C for 20 min. It was then directly used in the standard assay as a source of MraY activity (1 μL, final overall protein concentration ~1 mg/mL, final diamide concentration 50 μM). In both cases, fluorescence of the assay mixtures was measured over time (plate reader, 384-well plate format, λ_{ex} = 355 nm, λ_{em} = 520 nm). MraY activity at a specific inhibitor concentration was calculated by linear regression (0 to 2 min) and then plotted against logarithmic inhibitor concentrations (with sigmoidal fit to obtain IC_{50} values).

Antibacterial testing: Tests for antibacterial activity were performed as described before.[23a]

Acknowledgements

Parts of this work have been carried out within the framework of the SMART BIOTECS alliance between the Technische Universität Braunschweig and the Leibniz Universität Hannover. This initiative is supported by the Ministry of Science and Culture (MWK) of Lower Saxony, Germany. Financial support by the Deutsche Forschungsgemeinschaft (DFG, grants DU 1095/5-1 (C.D.) and KL 3012/2-1 (P.K.)) and the Fonds der Chemischen Industrie (FCI, P.K.) is gratefully acknowledged. The content of this work is solely the responsibility of the authors and does not necessarily represent the official views of the funding agencies. The authors thank the mass spectrometry unit, in particular Dr. Ulrich Papke, and the NMR spectroscopy unit of the Institute of Organic Chemistry at TU Braunschweig, in particular Dr. Kerstin Ibrom, for analytical support. Technical support by Nathalie Kagerah and Martina Jankowski (Saarland University) is also gratefully acknowledged. Open Access funding enabled and organized by Projekt DEAL.

Conflict of Interest

The authors declare no conflict of interest.

Data Availability Statement

Research data are not shared.

Keywords: enterobactin · Gram-negative bacteria · MraY · muraymycins · siderophore-drug conjugate

[1] a) M. A. Cooper, D. Shlaes, *Nature* **2011**, *472*, 32; b) D. I. Andersson, D. Hughes, *Nat. Rev. Microbiol.* **2010**, *8*, 260–271.
[2] a) T. J. Silhavy, D. Kahne, S. Walker, *Cold Spring Harbor Perspect. Biol.* **2010**, *2*, a000414; b) H. I. Zgurskaya, C. A. López, S. Gnanakaran, *ACS Infect. Dis.* **2015**, *1*, 512–522.
[3] a) H. Nikaido, *Cell Dev. Biol.* **2001**, *12*, 215–223; b) M. A. Webber, L. J. V. Piddock, *J. Antimicrob. Chemother.* **2003**, *51*, 9–11.
[4] R. C. Hider, X. Kong, *Nat. Prod. Rep.* **2010**, *27*, 637–657.
[5] a) P. Klahn, M. Brönstrup, *Nat. Prod. Rep.* **2017**, *34*, 832–885; b) Y.-M. Lin, M. Ghosh, P. A. Miller, U. Möllmann, M. J. Miller, *BioMetals* **2019**, *32*, 425–451; c) A. V. Cheng, W. M. Wuest, *ACS Infect. Dis.* **2019**, *5*, 816–828; d) M. J. Miller, R. Liu, *Acc. Chem. Res.* **2021**, *54*, 1646–1661.
[6] a) T. Zheng, E. M. Nolan, *J. Am. Chem. Soc.* **2014**, *136*, 9677–9691; b) P. Chairatana, T. Zheng, E. M. Nolan, *Chem. Sci.* **2015**, *6*, 4458–4471; c) W. Neumann, M. Sassone-Corsi, M. Raffatellu, E. M. Nolan, *J. Am. Chem. Soc.* **2018**, *140*, 5193–5201; d) C. Ji, P. A. Miller, M. J. Miller, *J. Am. Chem. Soc.* **2012**, *134*, 9898–9901; e) M. Ghosh, P. A. Miller, U. Möllmann, W. D. Claypool, V. A. Schroeder, W. R. Wolter, M. Suckow, H. Yu, S. Li, W. Huang, J. Zajicek, M. J. Miller, *J. Med. Chem.* **2017**, *60*, 4577–4583; f) R. Liu, P. A. Miller, S. B. Vakulenko, N. K. Stewart, W. C. Boggess, M. J. Miller, *J. Med. Chem.* **2018**, *61*, 3845–3854; g) L. Pinkert, Y. Lai, C. Peukert, S. Hotop, B. Karge, L. M. Schulze, J. Grunenberg, M. Brönstrup, *J. Med. Chem.* **2021**, *64*, 15440–15460; h) A. Sargun, T. C. Johnstone, H. Zhi, M. Raffatellu, E. Nolan, *Chem. Sci.* **2021**, *12*, 4041–4056; i) A. Sargun, M. Sassone-Corsi, T. Zheng, M. Raffatellu, E. M. Nolan, *ACS Infect. Dis.* **2021**, *7*, 1248–1259; j) E. Baco, F. Hoegy, I. J. Schalk, G. L. A. Mislin, *Org. Biomol. Chem.* **2014**, *12*, 749–757; k) Q. Perraud, P. Cantero, M. Munier, F. Hoegy, N. Zill, V. Gasser, G. L. A. Mislin, L. Ehret-Sabatier, I. J. Schalk, *Microorganisms* **2020**, *8*, 1820.
[7] a) H. Fiedler, P. Krastel, J. Müller, K. Gebhardt, A. Zeeck, *FEMS Microbiol. Lett.* **2001**, *196*, 147–151; b) S. M. Payne, I. B. Neilands, *Crit. Rev. Microbiol.* **1988**, *16*, 81–111.
[8] a) B. Ghysels, U. Ochsner, U. Möllman, L. Heinisch, M. Vasil, P. Cornelis, S. Matthijs, *FEMS Microbiol. Lett.* **2005**, *246*, 167–174; b) K. Poole, L. Young, S. Neshat, *J. Bacteriol.* **1990**, *172*, 6991–6996; c) C. R. Dean, S. Neshat, K. Poole, *J. Bacteriol.* **1996**, *178*, 5361–5369.
[9] P. Klahn, R. Zscherp, C. C. Jimidar, *Synthesis* **2022**, *54*, 3499–3557.
[10] a) P. Saha, B. S. Yeoh, R. A. Olvera, X. Xiao, V. Singh, D. Awasthi, B. C. Subramanian, Q. Chen, M. Dikshit, Y. Wang, C. A. Parent, M. Vijay-Kumar, *J. Immunol.* **2017**, *198*, 4293–4303; b) W. Zhu, M. G. Winter, L. Spiga, E. R. Hughes, R. Chanin, A. Mulgaonkar, J. Pennington, M. Maas, C. L. Behrendt, J. Kim, X. Sun, D. P. Beiting, L. V. Hooper, S. E. Winter, *Cell Host Microbe* **2020**, *27*, 376–388.
[11] R. Zscherp, J. Coetzee, J. Vornweg, J. Grunenberg, J. Herrmann, R. Müller, P. Klahn, *Chem. Sci.* **2021**, *12*, 10179–10190.
[12] a) C. Walsh, *Nat. Rev. Microbiol.* **2003**, *1*, 65–70; b) T. D. H. Bugg, D. Braddick, C. G. Dowson, D. I. Roper, *Trends Biotechnol.* **2011**, *29*, 167–173.
[13] a) G. Struve, F. C. Neuhaus, *Biochem. Biophys. Res. Commun.* **1965**, *18*, 6–12; b) J. S. Anderson, M. Matsuhashi, M. A. Haskin, J. L. Strominger, *Proc. Natl. Acad. Sci. USA* **1965**, *53*, 881–889; c) D. S. Boyle, W. D. Donachie, *J. Bacteriol.* **1998**, *180*, 6429–6432; d) M. G. Heydanek Jr, W. G. Struve, F. C. Neuhaus, *Biochemistry* **1969**, *8*, 1214–1221; e) A. Bouhss, D. Mengin-Lecreulx, D. Le Beller, J. Van Heijenoort, *Mol. Microbiol.* **1999**, *34*, 576–585; f) B. C. Chung, J. Zhao, R. A. Gillespie, D.-Y. Kwon, Z. Guan, J. Hong, P. Zhou, S.-Y. Lee, *Science* **2013**, *341*, 1012–1016.
[14] a) K. Kimura, T. D. H. Bugg, *Nat. Prod. Rep.* **2003**, *20*, 252–273; b) M. Winn, R. J. M. Goss, K. Kimura, T. D. H. Bugg, *Nat. Prod. Rep.* **2010**, *27*, 279–304.
[15] a) D. Wiegmann, S. Koppermann, M. Wirth, G. Niro, K. Leyerer, C. Ducho, *Beilstein J. Org. Chem.* **2016**, *12*, 769–795; b) L. A. McDonald, L. R. Barbieri, G. T. Carter, E. Lenoy, J. Lotvin, P. J. Petersen, M. M. Siegel, G. Singh, R. T. Williamson, *J. Am. Chem. Soc.* **2002**, *124*, 10260–10261; c) Z. Cui, X. Wang, S. Koppermann, J. S. Thorson, C. Ducho, S. G. Van Lanen, *J. Nat. Prod.* **2018**, *81*, 942–948.

[16] a) S. Koppermann, Z. Cui, P. D. Fischer, X. Wang, J. Ludwig, J. S. Thorson, S. G. Van Lanen, C. Ducho, *ChemMedChem* **2018**, *13*, 779–784; b) O. Ries, C. Carnarius, C. Steinem, C. Ducho, *MedChemComm* **2015**, *6*, 879–886; c) F. Graef, B. Vukosavljevic, J.-P. Michel, M. Wirth, O. Ries, C. De Rossi, M. Windbergs, V. Rosilio, C. Ducho, S. Gordon, C.-M. Lehr, *J. Controlled Release* **2016**, *243*, 214–224.
[17] a) T. Tanino, S. Ichikawa, M. Shiro, A. Matsuda, *J. Org. Chem.* **2010**, *75*, 1366–1377; b) K. Mitachi, B. A. Aleiwi, C. M. Schneider, S. Siricilla, M. Kurosu, *J. Am. Chem. Soc.* **2016**, *138*, 12975–12980.
[18] a) T. Tanino, S. Hirano, S. Ichikawa, A. Matsuda, *Nucleic Acids Symp. Ser.* **2008**, *52*, 557–558; b) A. P. Spork, S. Koppermann, B. Dittrich, R. Herbst-Irmer, C. Ducho, *Tetrahedron: Asymmetry* **2010**, *21*, 763–766; c) M. Büschleb, M. Granitzka, D. Stalke, C. Ducho, *Amino Acids* **2012**, *43*, 2313–2328; d) O. Ries, M. Büschleb, M. Granitzka, D. Stalke, C. Ducho, *Beilstein J. Org. Chem.* **2014**, *10*, 1135–1142.
[19] a) T. Tanino, S. Ichikawa, B. Al-Dabbagh, A. Bouhss, H. Oyama, A. Matsuda, *ACS Med. Chem. Lett.* **2010**, *1*, 258–262; b) T. Tanino, B. Al-Dabbagh, D. Mengin-Lecreulx, A. Bouhss, H. Oyama, S. Ichikawa, A. Matsuda, *J. Med. Chem.* **2011**, *54*, 8421–8439; c) Y. Takeoka, T. Tanino, M. Sekiguchi, S. Yonezawa, M. Sakagami, F. Takahashi, H. Togame, Y. Tanaka, H. Takemoto, S. Ichikawa, A. Matsuda, *ACS Med. Chem. Lett.* **2014**, *5*, 556–560; d) A. P. Spork, S. Koppermann, S. Schier, R. Linder, C. Ducho, *Molecules* **2018**, *23*, 2868.
[20] a) B. C. Chung, E. H. Mashalidis, T. Tanino, M. Kim, A. Matsuda, J. Hong, S. Ichikawa, S.-Y. Lee, *Nature* **2016**, *533*, 557–560; b) S. Koppermann, C. Ducho, *Angew. Chem.* **2016**, *128*, 11896–11898; *Angew. Chem. Int. Ed.* **2016**, *55*, 11722–11724.
[21] E. H. Mashalidis, B. Kaeser, Y. Terasawa, A. Katsuyama, D.-Y. Kwon, K. Lee, J. Hong, S. Ichikawa, S.-Y. Lee, *Nat. Commun.* **2019**, *10*, 2917.
[22] a) A. P. Spork, C. Ducho, *Org. Biomol. Chem.* **2010**, *8*, 2323–2326; b) A. P. Spork, D. Wiegmann, M. Granitzka, D. Stalke, C. Ducho, *J. Org. Chem.* **2011**, *76*, 10083–10098.
[23] a) A. P. Spork, M. Büschleb, O. Ries, D. Wiegmann, S. Boettcher, A. Mihalyi, T. D. H. Bugg, C. Ducho, *Chem. Eur. J.* **2014**, *20*, 15292–15297; b) D. Wiegmann, S. Koppermann, C. Ducho, *Molecules* **2018**, *23*, 3085; c) K. Leyerer, S. Koppermann, C. Ducho, *Eur. J. Org. Chem.* **2019**, 7420–7431; d) A. Heib, G. Niro, S. C. Weck, S. Koppermann, C. Ducho, *Molecules* **2020**, *25*, 22; e) G. Niro, S. C. Weck, C. Ducho, *Chem. Eur. J.* **2020**, *26*, 16875–16887.
[24] a) P. E. Brandish, K. Kimura, M. Inukai, R. Southgate, J. T. Lonsdale, T. D. H. Bugg, *Antimicrob. Agents Chemother.* **1996**, *40*, 1640–1644; b) P. E. Brandish, M. K. Burnham, J. T. Lonsdale, R. Southgate, M. Inukai, T. D. H. Bugg, *J. Biol. Chem.* **1996**, *271*, 7609–7614; c) T. Stachyra, C. Dini, P. Ferrari, A. Bouhss, J. van Heijenoort, D. Mengin-Lecreulx, D. Blanot, J. Biton, D. Le Beller, *Antimicrob. Agents Chemother.* **2004**, *48*, 897–902; d) S. Wohnig, A. P. Spork, S. Koppermann, G. Mieskes, N. Gisch, R. Jahn, C. Ducho, *Chem. Eur. J.* **2016**, *22*, 17813–17819.
[25] a) D.-C. Pöther, M. Liebeke, F. Hochgräfe, H. Antelmann, D. Becher, M. Lalk, U. Lindequist, I. Borovok, G. Cohen, Y. Aharonowitz, M. Hecker, *J. Bacteriol.* **2009**, *191*, 7520–7530; b) A. Müller, J. H. Hoffmann, H. E. Meyer, F. Narberhaus, U. Jakob, L. I. Leichertax, *J. Bacteriol.* **2013**, *195*, 2807–2816.
[26] Y. Terasawa, C. Sataka, T. Sato, K. Yamamoto, Y. Fukushima, C. Nakajima, Y. Suzuki, A. Katsuyama, T. Matsumaru, F. Yakushiji, S.-i. Yokota, S. Ichikawa, *J. Med. Chem.* **2020**, *63*, 9803–9827.

Manuscript received: August 2, 2022
Accepted manuscript online: October 12, 2022
Version of record online: December 5, 2022